Contributed paper

OPTO-ELECTRONICS REVIEW 7(4), 305–311 (1999)

512×512 element GeSi/Si heterojunction infrared focal plane array

H. WADA[1], M. NAGASHIMA[1], K. HAYASHI[1], J. NAKANISHI[2], M. KIMATA[2*], N. KUMADA[3], and S. ITO[3]

[1]Technical Research and Development Institute, Japan Defense Agency
1-2-24, Ikejiri, Setagaya, Tokyo 154-8511, Japan
[2]Advanced Technology R&D Center, Mitsubishi Electric Corporation
4-1, Mizuhara, Itami, Hyogo 664-8614, Japan
[3]Kamakura Works, Mitsubishi Electric Corporation, 325, Kamimachiya
Kamakura, Kanagawa 247-8520, Japan

We have developed a monolithic 512×512 element GeSi/Si heterojunction infrared focal plane array (FPA). The operation mechanism of the GeSi/Si heterojunction detector is the same as that of the PtSi/Si Schottky-barrier detector. We have fabricated the GeSi/Si heterojunction using molecular beam epitaxy (MBE) technology, and have confirmed that ideal strained GeSi films are grown on Si substrates. We have evaluated the dependencies of spectral responsivity on the Ge composition, impurity concentration and GeSi thickness, and have optimized them for 8-12 μm infrared detection. The 512×512 element FPA has a pixel size of 34×34 μm² and a fill factor of 59%. A low noise equivalent temperature difference of 0.08 K (f/2.0) was obtained with a 300 K background with a very small responsivity dispersion of 2.2%.

Keywords: MBE growth, GeSi/Si heterojunctions, focal plane arrays.

1. Introduction

Scanning imaging systems with linear detector arrays have been used for infrared imaging for a long time. Starting with the 3–5 μm spectral band, electronic imaging technology with 2-dimensional FPAs is spreading its application fields into the 8–12 μm spectral band. HgCdTe is a popular material for 8–12 μm infrared FPAs [1–3]. For compound semiconductors like the HgCdTe, the hybrid structure, where individual detectors are connected to silicon readout circuits via metal bumps, is indispensable. Serious thermal stress appears near the metal bumps during operation because the typical operating temperature of quantum detectors is about –200°C. As the number of elements in the FPA is increased, the chip size must be enlarged, and this increases the thermal stress. Thus, it is difficult to increase elements using the hybrid structure.

Operation mechanism of the GeSi/Si heterojunction infrared detector is the same as that of the PtSi/Si Schottky-barrier detector, which is the most advanced infrared imaging device in resolution. The GeSi/Si heterojunction infrared detector can be monolithically integrated on the same silicon substrate as that for readout circuits, and its cutoff wavelength can be tailored up to the 8–12 μm spectral region [4–7].

We have developed a high-resolution monolithic GeSi/Si heterojunction FPA for 8–12 μm imaging. In this paper, we will report on the spectral response and dark current of our GeSi/Si heterojunction detectors, and the effect on them of the Ge composition and impurity concentration. In addition to the study of these parameters, we will discuss the optimum GeSi film thickness. Finally, we will report on the design and performance of the 512×512 element GeSi/Si heterojunction FPA.

*e-mail: kimata@med.edl.melco.co.jp

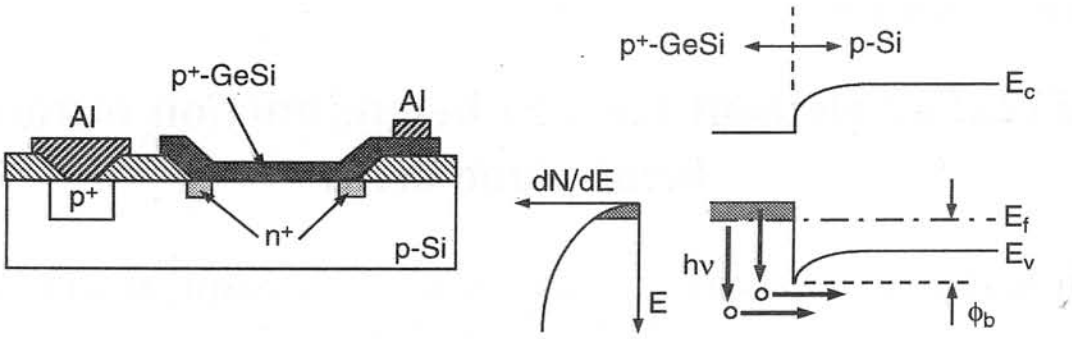

Fig. 1. Structure and operation of GeSi/Si heterojunction detector.

2. Structure and operation of detector

Figure 1 shows the structure and operation of the GeSi/Si heterojunction detector [5]. The structure is similar to that of the PtSi/Si Schottky-barrier detector except that the GeSi layer is replaced by the PtSi film. GeSi is a mixed crystal of Ge and Si, and its energy band gap can be tailored by varying the Ge composition. The GeSi film acts as an emitter. It is degenerately doped with boron, and a lot of holes populate in the upper states of the valence band as free carriers. When infrared rays strike the GeSi film, the holes are excited, and the exited holes are emitted into the Si if they have energy greater than the barrier height (ϕ_b) of the GeSi/Si heterojunction. This operation is called internal photoemission, which is familiar as the photodetection mechanism of the Schottky-barrier detector.

Cutoff wavelength is determined by the energy barrier

$$\lambda_c = \frac{1.24}{\Phi_b}, \tag{1}$$

where λ_c is the cutoff wavelength (μm), Φ_b is the barrier height (eV). Unlike the Schottky-barrier detector, Φ_b can be controlled by varying the Ge composition and boron concentration in the GeSi/Si heterojunction detector.

If the carrier movement in the GeSi film is assumed to be isotropic, the quantum efficiency is expressed as follows [7]

$$\eta = C_1 \frac{(h\nu - \Phi_b)^2}{h\nu}, \tag{2}$$

where η is the quantum efficiency (electrons/photon), C_1 is the quantum efficiency coefficient (eV^{-1}), h is the Planck constant (eVs), and ν is the frequency (Hz).

Quantum detectors are cooled in order to reduce the dark current and to increase the signal-to-noise ratio. The operating temperature of the detectors in decided by considering the temperature dependence of the dark current. The dark current of the GeSi/Si heterojunction detector is dominated by the thermionic emission current, as is that of the Schottky-barrier detector, and is given by

$$J_D = AT^2 \exp\left(-\frac{\Phi_b}{kT}\right), \tag{3}$$

where J_D current density (A/cm^2), A is the Richardson constant (A/cm^2K^2), T is the operating temperature (K), and k is the Boltzmann constant (J/K).

3. Manufacturing of GeSi/Si heterojunction

The GeSi/Si heterojunction is fabricated by growing a GeSi film on a (100) p–Si substrate using molecular beam epitaxy (MBE) technology. Figure 2 shows a cross-sectional transmission electron micro-

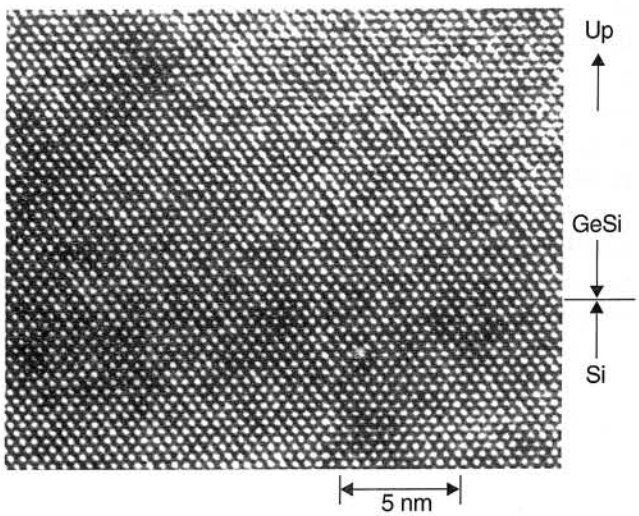

Fig. 2. Cross-sectional TEM image of GeSi film.

scope (TEM) image of a 20 nm GeSi film with a Ge composition of 0.4 and boron concentration of 2×10^{20} cm^{-3}.

The lattice constant of Ge is 4% larger than that of Si. Thus, when the GeSi film is thin, the strained GeSi film matches its own lattice constant with that of the Si substrate as the film is grown. But, when the thickness of the GeSi film exceeds the critical thickness, the lattice of the GeSi film is relaxed with dislocations which degrade the electrical characteristics of the junction. To obtain good GeSi/Si heterojunctions, it is important to grow GeSi films with the strained structure. Figure 2 shows that our GeSi film has an ideal strained structure.

4. Performance of GeSi/Si heterojunction

To evaluate the performance of our GeSi/Si heterojunctions, we manufactured 600×400 μm^2 photodetectors.

4.1. Spectral response

Figure 3 shows the dependence of the spectral response on the Ge composition. The responsivity calculated from Eq. (2) becomes smaller as the wavelength becomes longer. However, the responsivity in Fig. 3 is almost constant in the short wavelength region. The reason for this characteristic is small absorptivity of the GeSi film in the short wavelength region. In the longer wavelength region, the responsivity decreases as the wavelength increases. The cutoff wavelength is defined as the wavelength where the responsivity becomes 0, and it is obtained by extrapolating data in the long wavelength region.

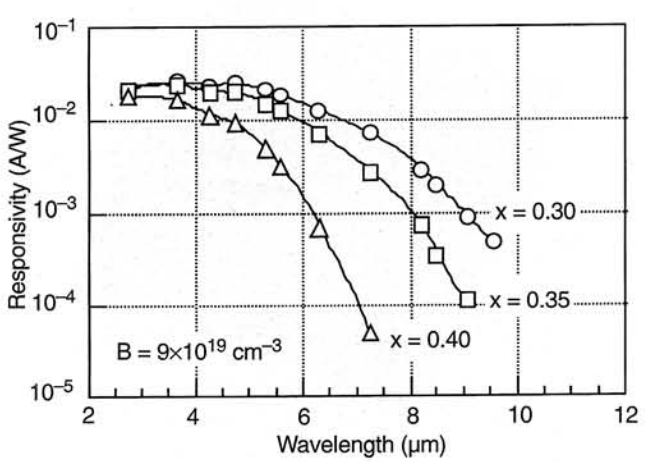

Fig. 3. Dependence of spectral response on Ge composition.

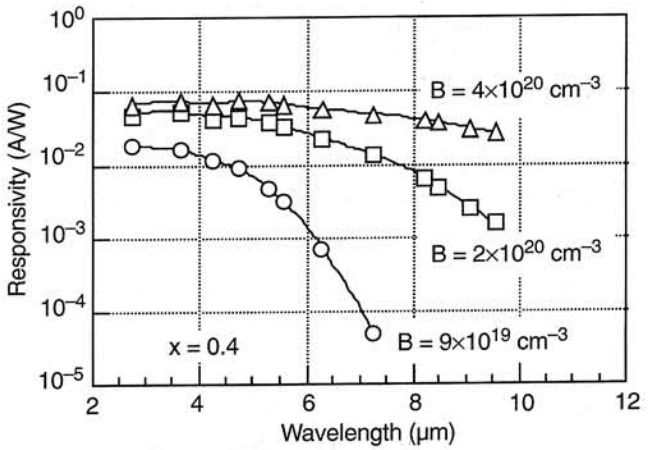

Fig. 4. Dependence of spectral response on boron concentration.

The spectral response depends on the Ge composition, reflecting the dependence of the barrier height on the Ge composition. As the Ge composition becomes smaller, the cutoff wavelength becomes longer.

Figure 4 shows the dependence of the spectral response on the boron concentration. Higher boron concentration gives longer cutoff wavelength because the Fermi level moves deeply into the valance band when boron concentration is increased.

Figure 5 shows the dependence of the barrier height on the Ge composition, and Fig. 6 shows the dependence of the quantum efficiency coefficient (C_1) on the boron concentration. The small dependence of the barrier height on the Ge composition for a boron concentration of 4×10^{20} cm^{-3} and the decrease in the quantum efficiency coefficient in the higher boron concentration region indicate that too much boron concentration damages the strained structure and degrades the detector performance.

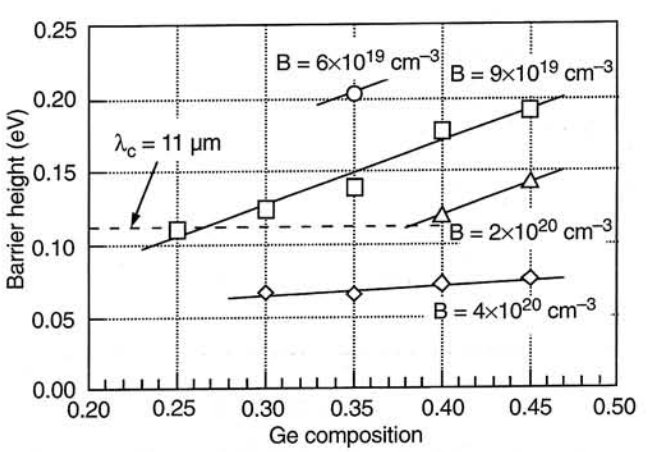

Fig. 5. Dependence of barrier height on Ge composition.

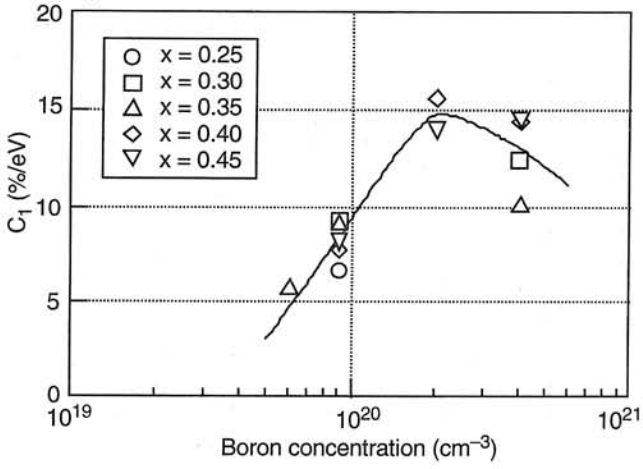

Fig. 6. Dependence of quantum efficiency coefficient on boron concentration.

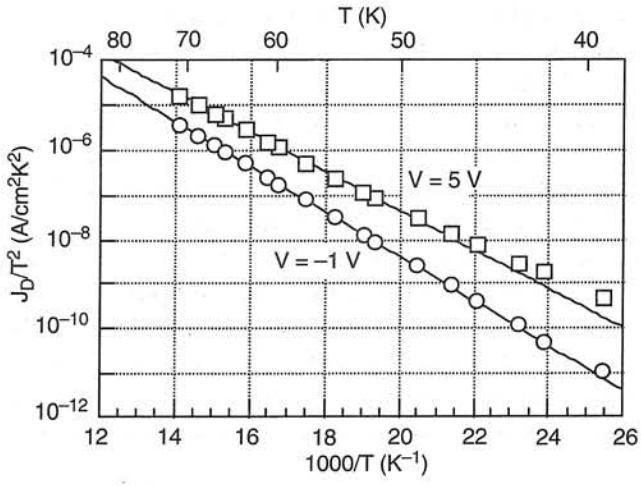

Fig. 8. Dependence of dark current on temperature.

4.2. Optimization of GeSi thickness

Figure 7 shows the dependence of the quantum efficiency coefficient on the GeSi thickness. This dependence is explained by considering the effect of infrared absorption in the GeSi film and the effect of multiple reflection of excited hot carriers in the GeSi film. While thicker GeSi film absorbs more infrared energy than thinner film, enhancement by multiple reflection is less effective in the former than in the latter. So the GeSi heterojunction detector has an optimum GeSi thickness at which the quantum efficiency is maximized. From the result shown in Fig. 7, the optimum GeSi thickness of our detector was determined to be 20 nm.

4.3. Dark current

Figure 8 shows the dependence of the dark current on temperature. In this figure, the x-axis is the inverse of the operating temperature. The characteristics are in good agreement over a wide range of operating temperatures with the thermionic emission theory expressed by Eq. (3).

5. 512×512 element GeSi/Si heterojunction infrared FPA

We have developed a 512×512 element GeSi/Se heterojunction infrared FPA with the following GeSi formation parameters.

- Ge composition: 0.4,
- Boron concentration: 2×10^{20} cm^{-3},
- GeSi thickness, 20 nm.

Figures 9, 10, and 11 show a photograph of the image sensor, the pixel cross section, and a scanning electron mocroscope (SEM) photograph of the pixels, respectively. The pixel size is 34×34 μm^2, and the fill factor is 59%. The chip size is 20.6×19.4 mm^2.

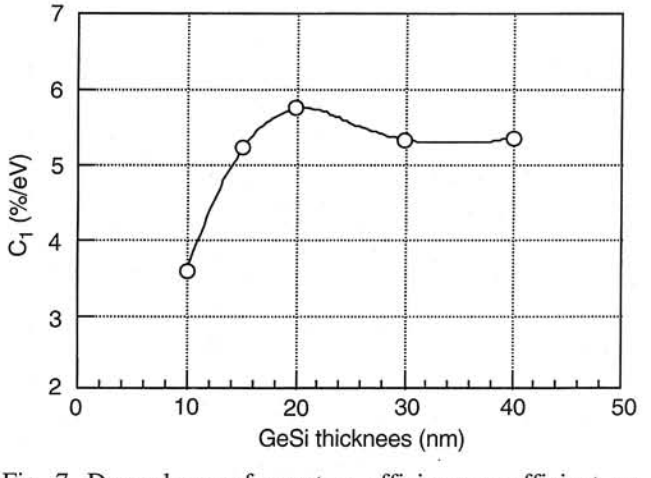

Fig. 7. Dependence of quantum efficiency coefficient on GeSi thickness.

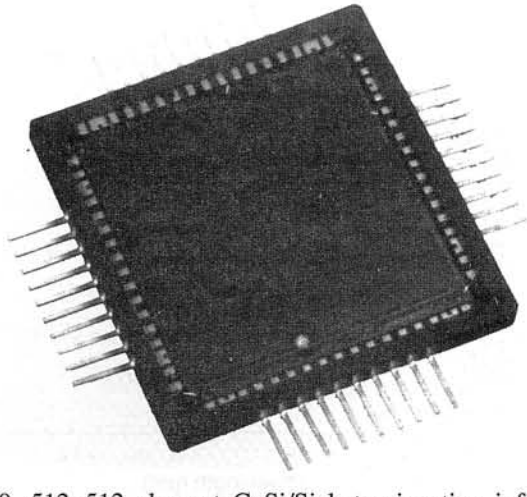

Fig. 9. 512×512 element GeSi/Si heterojunction infrared FPA.

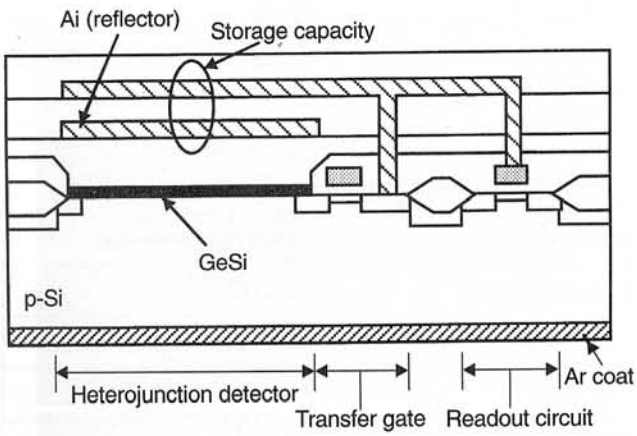

Fig. 10. Pixel cross section.

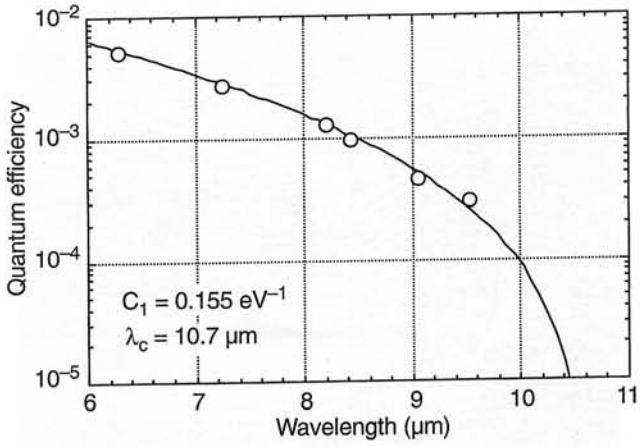

Fig. 12. Spectral response of FPA.

We chose a MOS readout architecture because the transfer efficiency of the CCD is seriously degraded at 40–50 K operating temperatures of GeSi heterojunction FPAs for the 8–12 μm spectral band. Signal charge is stored in the detector during the integration time. The storage charge is transferred to a storage capacitor, which is stacked over the detector as shown in Fig. 10, and the voltage change at the storage capacitor is read out through a source follower circuit at the pixel. We adopted a 2:1 interlace readout mode in this FPA.

Figure 13 shows the spectral response of the FPA. The solid line in this figure is a curve calculated using Eq. (2) with a quantum efficiency coefficient of 0.155 eV^{-1} and cutoff wavelength of 10.7 μm.

Figure 12 shows the histogram of the responsivity in our FPA. The standard deviation of 64×64 elements in the center is 2.2% of the average responsivity. The number of defective elements is 4 elements out of 500×500 elements; thus, the proportion of defects is less than 0.002%. A defective element is defined as an element the responsivity of which exceeds ±50% of the average responsivity. Considering our experience with the production of 1040×1040 element PtSi Schottky-barrier FPAs, it should not be too difficult to obtain 512×512 element GeSi FPAs with no defects when we have mastered the GeSi FPA production process.

6. Imaging performance

We have evaluated imaging performance of our FPA. Figure 14 shows an overview of the imager. Refraction type f/2.0 optics is used for this imager. The FPA is operated at a frame rate of 30 Hz. The field-of-view is 6°×6°. The operation temperature of the FPA is 43 K.

The image signal from the FPA is processed in offset and gain correction circuits, and is output as an RS-170 standard video signal. Figure 15 is video output for 32°C and 22°C blackbody targets. A 10 K temperature difference yields a 290 mV video signal, and the resulting differential temperature response is 29 mV/K. Since the video noise at 300 K is measured as 14 mV peak-to-peak, the noise equivalent tempera-

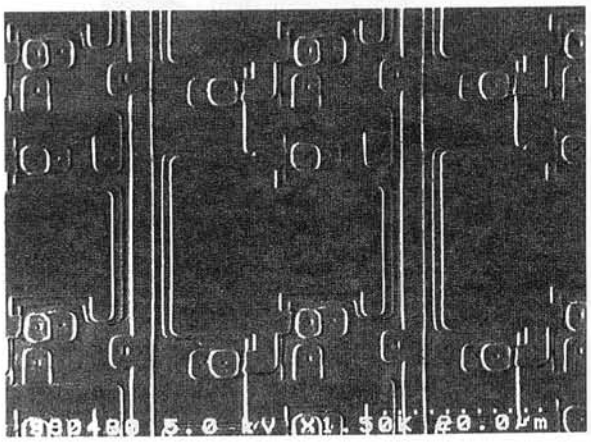

Fig. 11. SEM photograph of pixel.

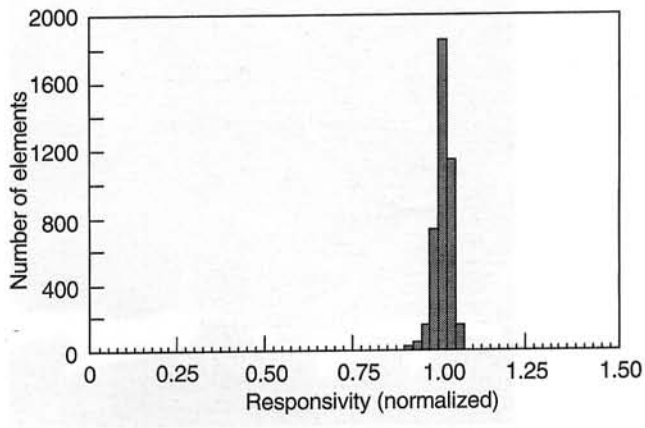

Fig. 13. Histogram of relative responsivity.

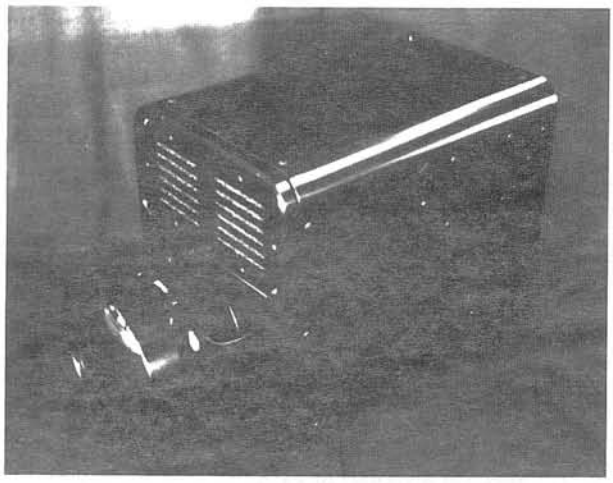

Fig. 14. Overview of imager.

ture difference (NETD) is 0.08 K. Dynamic range (D/R) is defined as the ratio of the display temperature range to NRTD. In this imager, the display temperature range is 46°C, so D/R is about 55 dB.

Table 1 shows the specifications and typical performance of the imager, and Fig. 16 shows some examples of thermal images with this imager.

Table 1. Specifications and performance of imager

Detector	GeSi/Si heterojunction
Array size	512×512
Pixel size	34×34 μm^2
Fill factor	59%
Readout	MOS architecture
Dispertion	2.2% (non-corrected)
Defect	< 0.002%
NETD	0.08 K (f/2.0, 300 K)
Dynamic range	55 dB

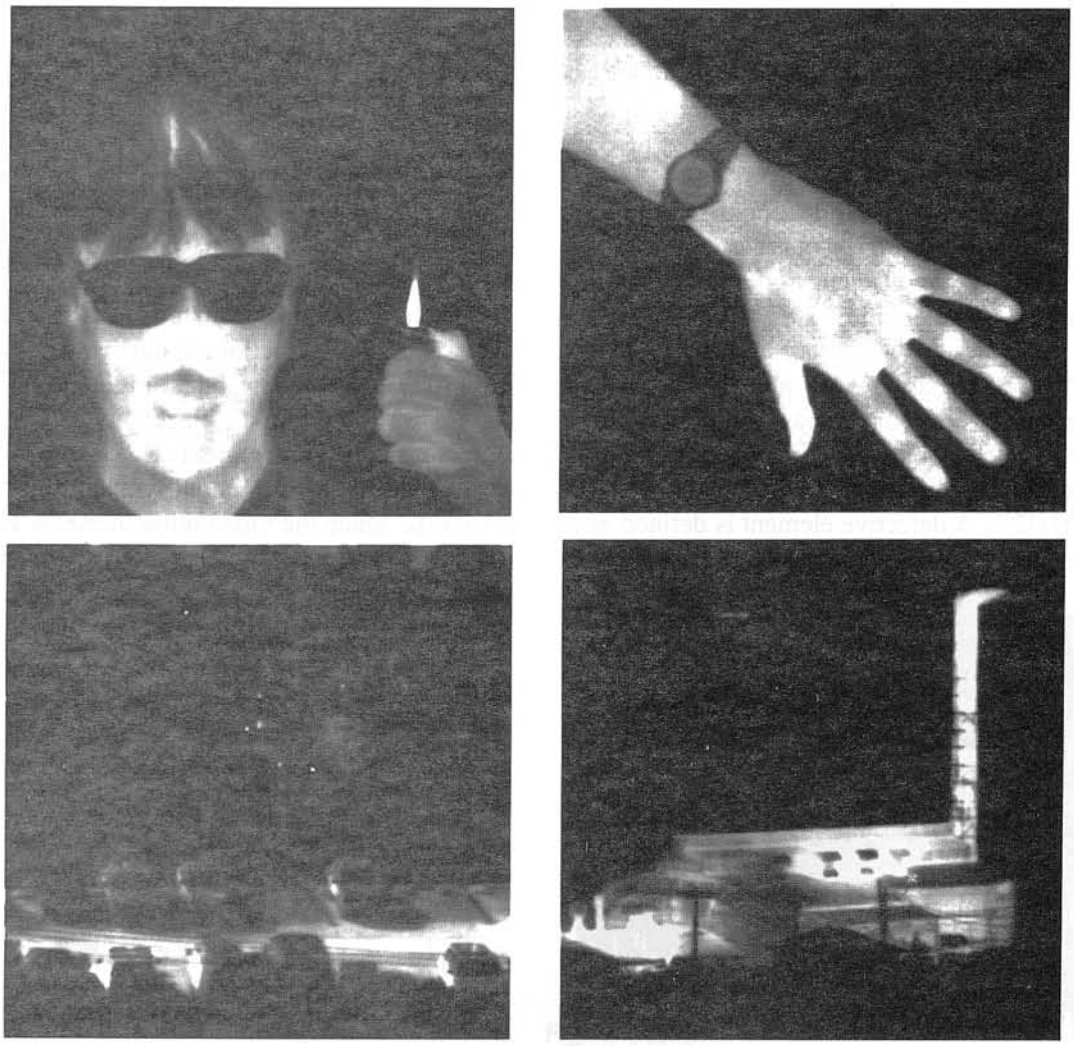

Fig. 15. Video outputs for 32°C and 22°C balackbody targets.

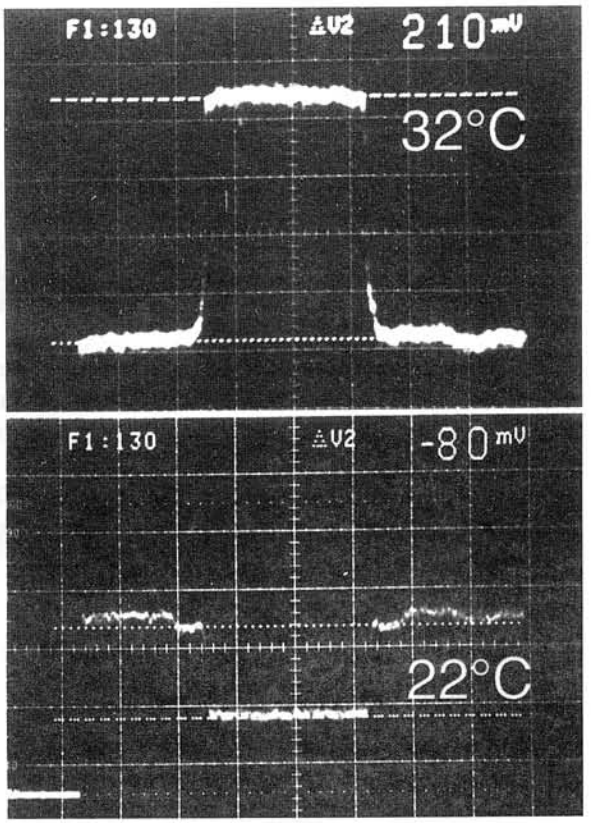

Fig. 16. Examples of thermal images.

7. Conclusion

In order to realize high performance GeSi/Si heterojunction FPAs, we have evaluated the dependencies of spectral responsivity on the Ge composition, impurity concentration and GeSi thickness, and have optimized them for 8–12 μm infrared detection. We have developed a monolithic 512×512 element GeSi/Si heterojunction infrared FPA. The FPA has a pixel size of 34×34 μm^2 and a fill factor of 59%. In preliminary evaluation, we have obtained a low noise equivalent temperature difference of 0.08 K (f/2.0) with a 300 K background and a dynamic range of 55 dB with a very small responsivity dispersion of 2.2% and high pixel yield of 99.998%.

References

1. T. Kanno, M. Saga, A. Kawashima, R. Oikawa, A. Ajisawa, Y. Tomioka, N. Oda, T. Yamagata, S. Murashima, T. Shima, and N. Tasuda,"Development of MBE-grown HgCdTe 64×64 FPA for long-wavelength IR detection", *Proc. SPIE* **2020**, 41–48 (1993).
2. T. Kanno, M. Saga, N. Kajiwara, K. Awamoto, G. Sudo, Y. Ito, and H. Ishizaki,"Development of LPE-grown HgCdTe 64×64 FPA with a cut-off wavelength of 10.6 μm", *Proc. SPIE* **2020**, 49–56 (1993).
3. K. Kanno, H. Wada, M. Nagashima, H. Wakayama, K. Awamoto, N. Kajiwara, Y. Ito, and M. Nakamura,"256×256 element HgCdTe hybrid IRFPA for the 8-10 μm band", *Proc. SPIE* **2552**, 384–391 (1995).
4. T.L. Lin, E.W. Jones, A. Ksendzov, S.M. Dejewski, R.W. Fathauer, T.N. Krabach, and J. Majserian.,"A novel Si-based LWIR detector: The SiGe/Si heterojunction internal photoemission detector", *Tech. Digest of IEDM*, 641–644 (1990).
5. B.Y. Tsaur, C.K. Chen, and S.A. Marino, "Long-wavelength Ge_xSi_{1-x}/Si heterojunction infrared detectors and focal plane array", *Proc. SPIE* **1540**, 580–595 (1991)
6. T.L. Lin, T. George, E.W. Jones, A. Ksendzov, and H.L. Huberman, "Elemental boron-doped p^+-SiGe layers grown by molecular beam epitaxy for infrared detector applications", *Appl. Phys. Lett.* **60**, 380–382 (1992).
7. T.L. Lin, J.S. Park, S.D. Gunapala, E.W. Jones, and H.M. Del Castillo, "Photoresponse model for $Si_{1-x}Ge_x$/Si heterojunction internal photoemission infrared detector", *IEEE Electron Device Lett.* **15**, 103–105 (1994).